Optics Communications 331 (2014) 82–86

Contents lists available at ScienceDirect

Optics Communications

journal homepage: www.elsevier.com/locate/optcom

Projection two-photon polymerization using a spatial light modulator

Liang Yang, Jiawen Li *, Yanlei Hu *, Chenchu Zhang, Zhaoxin Lao, Wenhao Huang, Jiaru Chu

Department of Precision Machinery and Precision Instrumentation, University of Science and Technology of China, Hefei 230026, PR China

ARTICLE INFO

Article history:
Received 3 March 2014
Received in revised form
13 May 2014
Accepted 22 May 2014
Available online 9 June 2014

Keywords:
Femtosecond laser
Two-photon polymerization
Spatial light modulator
Parallel fabrication

ABSTRACT

The development of a high-efficiency projection two-photon polymerization (P2PP) process by using a liquid crystal spatial light modulator (SLM) is presented. Rapid fabrication of 2D patterned microstructures with P2PP is demonstrated, and the effect of laser pattern and exposure dose on the surface roughness of the fabricated microstructures is investigated. It is found that the distribution of laser intensity at the focal plane of objective has a significant effect on the profiles of microstructures. This unique technology has a promising approach to increase the efficiency of two-photon polymerization (2PP) and a parallel fabrication of complex 2D and 3D microstructures.

1. Introduction

2PP is a powerful tool that uses tightly focused high-intensity laser to produce highly localized nonlinear light–matter interaction inside a photosensitive material [1]. Due to the nonlinear nature of 2PP, this technique has a scalable resolution of hundreds of nanometers down to sub-100 nm [2–4]. The most remarkable property is that the network of precisely overlapped voxels can permit fabrication of delicate 3D microstructures with arbitrary shape. These properties make 2PP an appealing technique for the fabrication of functional micro/nanodevices [5–10].

While this technique can produce extremely high-resolution 3D structures, it has a major drawback of low efficiency due to the serial nature of the point-by-point processing. It may take hours to fabricate a single micro/nanodevice [11]. This significantly obstructs the development of 2PP technology. Due to this point, 2PP has been primarily limited to academic applications. Therefore, those involved in the 2PP field would appeal for further research into the area of parallel 2PP technique. Jun-ichi Kato et al. introduced a mircolens array into the 2PP fabrication system to separate femtosecond laser into tens or even hundreds of spots for parallel fabrication [12]. Similarly, Xianzi Dong et al. split a femtosecond laser beam into multiple beams with diffractive optical elements [13]. However, with the microlens array or diffractive optical elements method, the distribution of the foci is related with the design of the microlens array and diffractive optical elements. The locations of specified foci are fixed and unadjustable. Other techniques involve holographic lithography [14,15] and use of specifically shaped beams [16,17]. Nevertheless, with these methods, only microstructures with specific periods or specific profiles can be fabricated. Recently, SLM was introduced into the 2PP fabrication system where femtosecond laser beam was modulated into multilaser spots and tightly focused into materials for parallel fabrication [18–22]. This technique significantly increased the speed of 2PP. However, microstructures were still fabricated by the scanning of individual laser spots and the flexibility of SLM based 2PP was not fully investigated. A digital mirror device (DMD) based lithography technique was also demonstrated recently [23,24]. Parallel processing of complex structures was realized by spatially shaping the intensity profile of incident laser pulse using DMD. However, DMD modulates the light by controlling micromirror arrays to switch the light on and off at each individual pixel [24–26]. So only the laser reflected from the switched on mirror is used, which sometimes accounts for only a small percentage of the whole mirror array. In fact, the usable power is especially important in the 2PP system since there exists a threshold power for 2PP. Besides, DMD can modulate light beam into only 2D patterns, whereas 3D laser pattern can be expected by phase modulation using a liquid crystal SLM, which is used in this research.

This paper continues the research in SLM-based 2PP and DMD-based lithography [18,24], presenting the development of a high-efficiency P2PP process by using a liquid crystal SLM. A P2PP system based on SLM is built. A femtosecond laser beam is modulated to diverse 2D patterns and then focused into a photoresist with an objective lens for parallel fabrication. The fabrication of microstructures is investigated based on the exposure dose and

* Corresponding authors.
E-mail addresses: jwl@ustc.edu.cn (J. Li), huyl@ustc.edu.cn (Y. Hu).

http://dx.doi.org/10.1016/j.optcom.2014.05.051
0030-4018/

the laser pattern. It is hoped that this research could form a foundation for the further development of P2PP technique.

2. Experiment

2.1. Principle

In traditional 2PP fabrication, femtosecond laser beam is attenuated and then focused directly into photoresists to fabricate microstructures serially in line and in layer with a single laser spot [11]. However, in this experiment, a SLM is added to 2PP fabrication system and a high-efficiency P2PP apparatus is developed. Laser beam illuminating the SLM is shaped to specific patterns according to the loaded computer generated holograms (CGHs) and then the modulated laser beam is focused by an objective into curable photoresist. The illuminated area is solidified by 2PP and the patterns are formed simultaneously in the photoresist under one shot.

2.2. System overview

The P2PP system is schematically illustrated in Fig. 1. The femtosecond laser source used in the experiment (Coherent Chameleon) has 75 fs pulse width, 80 MHz repetition rate and 800 nm center wavelength. The power of femtosecond laser is 2.2 W and is attenuated with a half wave plate combined with a Glan laser beamspliter. After passing through a beam expander, the laser beam illuminates a phase only SLM (Holoeye Pluto NIRII) which is suitable for wavelength from 700 nm to 1000 nm. To achieve better modulation effect, the expanded laser beam slightly overfills the SLM displayer. By loading CGHs to the SLM, the first-order diffracted femtosecond laser beam forms arbitrarily designable patterns at the Fourier plane P. The other diffraction orders created by the SLM are blocked with a spatial filter. The modulated femtosecond laser pattern is then focused into photoresists with an objective for 2PP. The photoresists used in the experiment are IP-L (Nanoscribe) and SU-8 2075 (Microchem), both commercial. IP-L is drop-casted between two cover glasses spaced with adhesive plaster and then anchored to a 3D piezo-stage (Physik Instrument E545). The adhesive plaster is more than 100 μm thick, which is thick enough to make sure that 2PP happens in the inner part of photoresists. SU-8 is prepared and developed according to the standard guidelines. The process of fabrication is monitored in situ with a CCD camera.

SLM is the core component of a P2PP system, which is used in areas such as laser pulse shaping [27], optical trapping [28], and parallel ablation of metal surface [29]. The SLM used here is a Holoeye Pluto NIRII, which is used for controlling an LCOS (Liquid Crystal-on-Silicon) active matrix reflective mode phase only liquid crystal displayer with 1920 × 1080 resolution and 8 μm pixel pitch. This device is frequently used in displaying real-time CGHs. CGHs that act as phase controlling holograms with 256 Gy levels are used here. The CGHs are generated with the Gerchberg–Saxton (GS) algorithm, an iterative 2D Fourier transform algorithm [28].

3. Results and discussion

3.1. P2PP with femtosecond laser modulated to curve patterns

The P2PP is demonstrated in Fig. 2. The insets of Fig. 2 show the target laser patterns where white corresponds to laser light and black corresponds to absence of laser light. The patterns include letters (“U”, “S”, “T”, “C”), triangle pattern and circle pattern, which we together called curve patterns. The designed patterns are in the region of 100 × 100 pixels in SLM display panel. By loading the calculated CGHs to SLM, femtosecond laser is modulated to corresponding curve patterns and then focused into photoresists with a 63 × objective (NA = 1.4). In contrast to projection micro-stereolithography [25,26] the innate chemical process of P2PP is two-photon absorption and therefore polymerization can be aroused only near the focus of laser beam, not all along the beam path.

The first order of the diffraction beam from SLM has a maximum power of 560 mW in our system. There is a power threshold for 2PP and if the laser density in the designed laser pattern is lower than the threshold, 2PP will not develop. Fig. 3 shows the results of P2PP with 100 × objective in SU-8 photoresist. The total power of T-shaped laser beam is 560 mW. The exposure times of Fig. 3(a)–(d) are 5 s, 1 s, 500 ms, 200 ms in order. As seen in the figure, the T-shaped microstructure becomes less and less complete with the decrease of exposure time. The further decrease of exposure time will fail 2PP. Since the average laser power that corresponds to each pixel in the designed laser pattern is low, the exposure time of P2PP is much longer than that of the normal single spot 2PP. If the usable power of P2PP system is increased, 2PP can be aroused as fast as that of normal single spot 2PP. So, the usable power is a crucial factor of a P2PP system to decide the efficiency of P2PP. In Fig. 3(c) and (d), it can be seen that only some parts of the pattern survive the decrease of laser power. This shows that the power distribution of laser pattern is not uniform. The exposure time, which should be appropriately selected, significantly affects the quality of fabricated patterns.

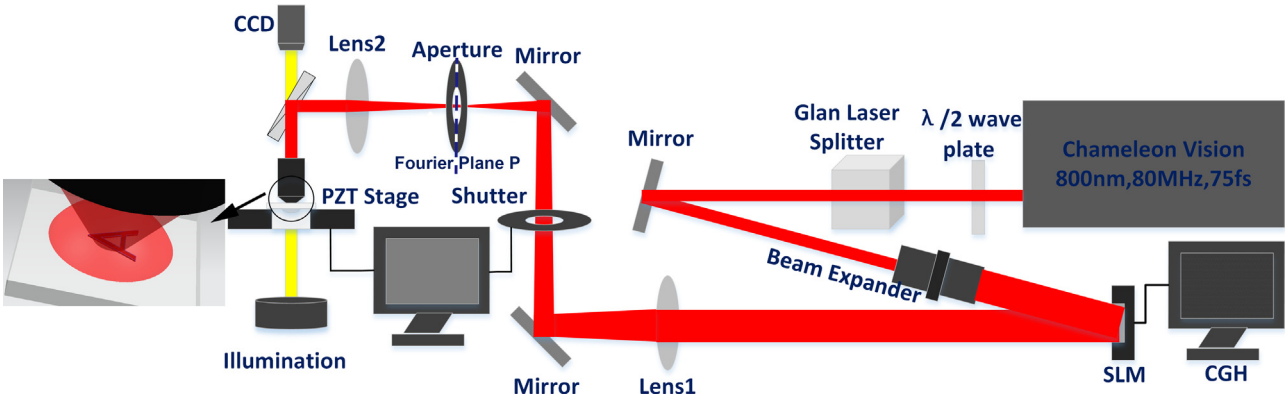

Fig. 1. Schematic illustration of projection 2PP system. Inset: laser pattern focused into the photoresist.

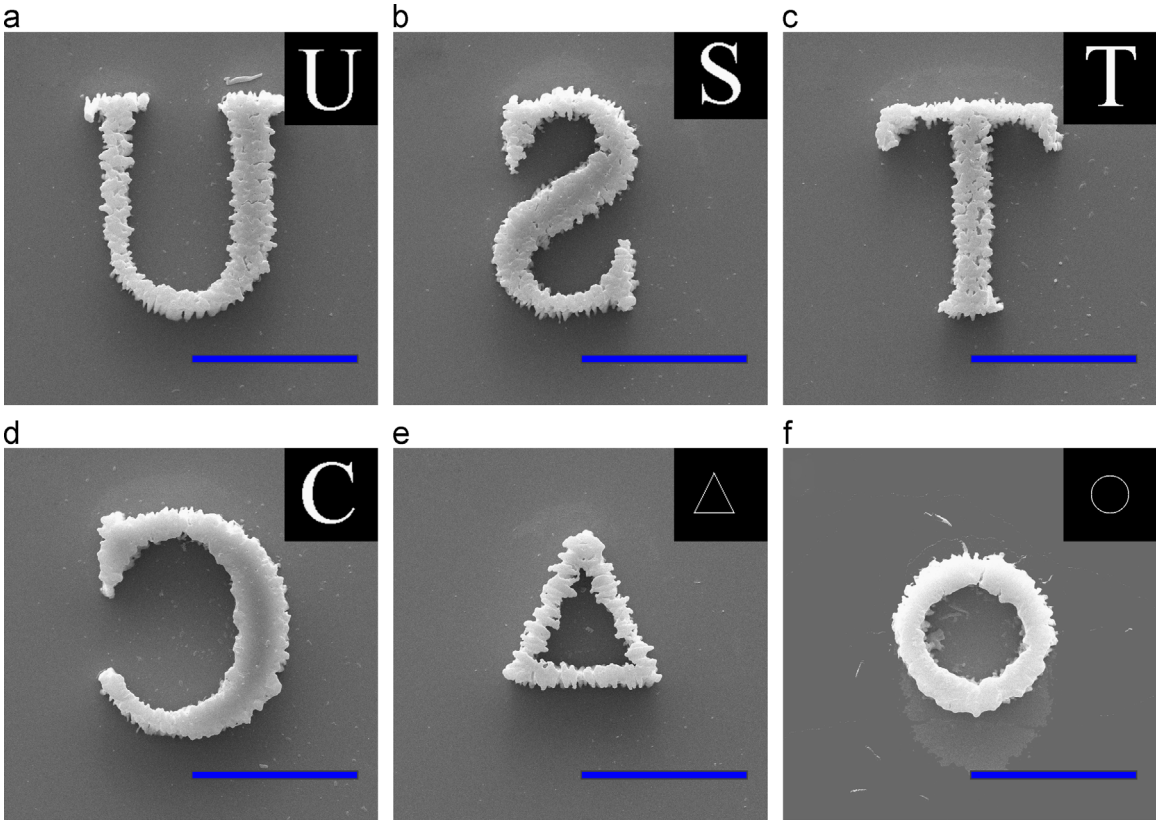

Fig. 2. Femtosecond laser reflected from the SLM is modulated to curve patterns and then focused into the photoresist with a 63 × objective (NA = 1.4) for 2PP. The insets are the designed curve patterns. All the scale bars are 30 μm.

3.2. P2PP with femtosecond laser modulated to plane patterns

In addition to P2PP with curve patterned laser beam, P2PP with plane patterned laser beam is also investigated. Femtosecond laser beam is modulated to circle plane, square plane and triangular plane, and then focused into photoresists for 2PP fabrication. The SEM images of the fabricated structures are shown in Fig. 4(a)–(c). The designed laser pattern in Fig. 4(a) has a diameter of 20 pixels. The designed laser patterns in Fig. 4(b) and (c) have a side length of 20 pixels. In this research, IP-L is used as the photoresist with 50 × objective (NA = 0.8). As shown in Fig. 4, circle, square and triangular microstructures are obtained.

It is obvious that the top of the obtained microstructures is relatively smooth. To find out whether they can still stay smooth when the white points of the designed pattern are not continuous, further experiments are conducted. In Fig. 4(d)–(f), femtosecond laser beam is modulated to plane patterns with certain distance between laser spots. In Fig. 4(d), there are 20 white points in the diameter with an interval of 1 pixel. There are 20 white points and 40 white points at the side of the square plane in Fig. 4(e) and (f), respectively, and the interval of white points is also 1 pixel. The top of the microstructures is still smooth.

To further investigate how the surface roughness is affected by the fabrication parameters of P2PP, a series of experiments are done by changing the exposure time and the pixel intervals of 20 × 20 laser spots. The roughness of the top of microstructures are measured with an optical profiler (Wyko NT 1100). The results are shown in Fig. 5. As seen in the figure, with a certain exposure time, the surface roughness of microstructures decreases with the decrease of the laser spots interval. When the interval is fixed, the surface roughness of microstructure decreases remarkably with an increase of exposure time.

In conventional 2PP fabrication with single laser spot, 3D structures are constructed by individual voxels with lateral size of tens of nanometers. Thus, the edges of 3D structures are rather sharp and smooth. However, the edge of plane pattern is not so sharp that causes deformation. This is due to the intensity distribution of laser pattern not being uniform, especially at the edge of laser pattern. In conventional 2PP fabrication, the height of a single voxel can be about 200 nm. The 3D structures can be prototyped every 200 nm. However, in this case, the heights of polymerized microstructures are over 20 μm. Although the height depends on the laser pattern and the processing parameters, it is generally much larger than that of the conventional single voxel. This is a significant difference between P2PP and conventional 2PP. Another difference is that the average power for a laser spot to arouse 2PP is lower when P2PP technique compared to conventional 2PP technique. Here, 2PP can still be aroused with 40 × 40 laser spot while the average power of a laser spot is 0.35 mW (Fig. 4(f)). However, the threshold power to arouse 2PP in conventional 2PP technique with our system is measured to be approximately 6 mW.

To illustrate the profile and surface roughness of polymerized structure by P2PP, it is necessary to discuss the laser intensity distribution at the focal plane and the process of polymerization. Therefore, a semiquantitative analysis is conducted in this research. The distance between polymerized voxels l is linearly related to the interval of pixels Δd in the designed laser pattern and can be obtained as follows:

$$l = \frac{\lambda f_1}{d_{\text{pixel}} N_{\text{pixel}}} \Delta d \frac{f_{\text{objective}}}{f_2} \tag{1}$$

where λ is the wavelength of light source, f_1 and f_2 are the focal length of lens1 and lens2 behind SLM, respectively, $f_{\text{objective}}$ is the focal length of objective, $d_{\text{pixel}}$is the period of pixels on the

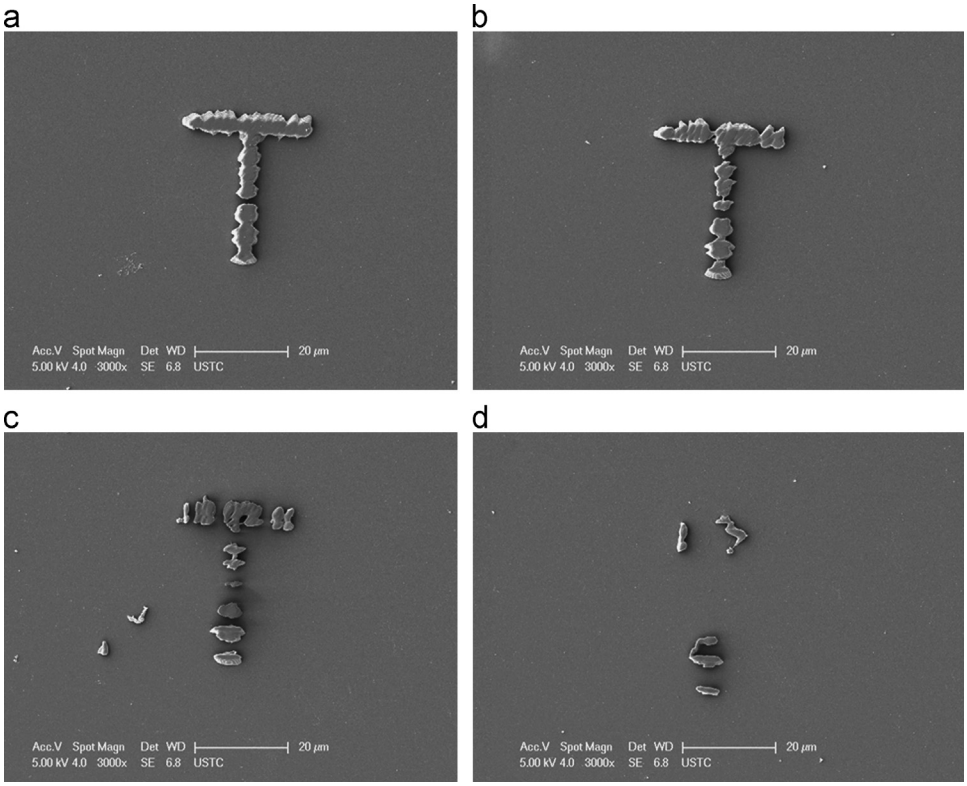

Fig. 3. Microstructures fabricated with T-shaped femtosecond laser beam. The power of the T-shaped laser beam is 560 mW. The exposure time of (a), (b), (c) and (d) is 5 s, 1 s, 0.5 s, and 0.2 s respectively.

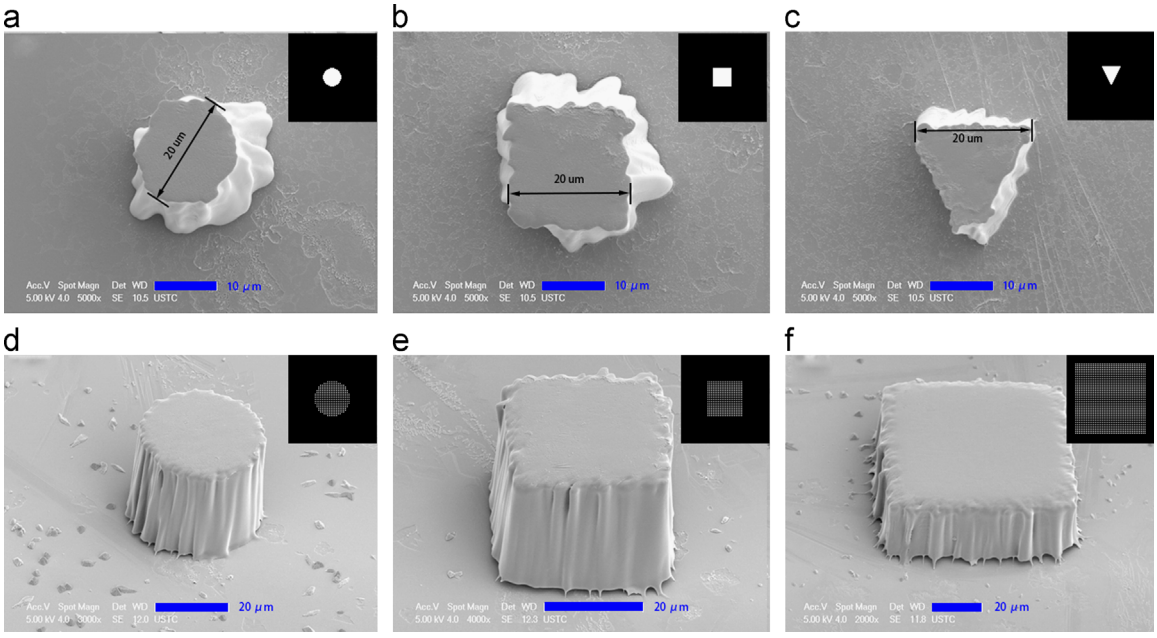

Fig. 4. Femtosecond laser reflected from the SLM was modulated to circle/square/triangular plane and then focused into the photoresist for 2PP; (a)–(c) SEM images of the results of P2PP with continuous pixel laser patterns. The scale bars are 10 μm; (d)–(f) SEM images of the results of P2PP with discontinuous pixel laser pattern. The scale bars are 20 μm.

displayer of SLM and N_{pixel} is the number of used pixels in one direction. To achieve better resolution of P2PP, shorter wavelength of laser source and shorter focal length of lens1 as well as objective should be chosen while longer focal length of lens2 should be selected for a fixed SLM. In our system, λ is 800 nm; f_1, $f_2$are 600 mm and 200 mm respectively. The focal length of a 50 × objective $f_{\text{objective}}$ is 3.6 mm; d_{pixel} is 8 μm and N_{pixel} is 1080. Hence, 1 pixel in the laser pattern corresponds to a size of 1 μm in the photoresist. This fits well with the size of the microstructures as shown in Fig. 4.

It is assumed that the resin is polymerized as soon as the particle density of radicals,$\rho(x,y,z)$, exceeds a certain threshold value ρ_{th}. The density of radicals, ρ, can be calculated from the below equation:

$$\rho(x,y,z) = [1-\exp(-\delta t I^2)]\rho_0 \tag{2}$$

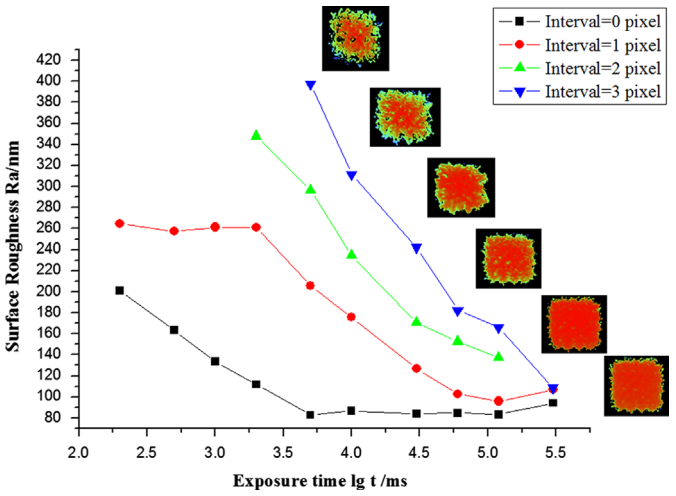

Fig. 5. Surface roughness of the fabricated structures versus exposure time and pixel distance. The power of laser beam is 560 mW and a 50 × objective (NA=0.8) is used in the experiments. Material used here is IP-L photoresist.

where $\delta$is the effective two-photon cross section, ρ_0 is the primary initiator particle density, $t$is the exposure time and $I$is the distribution of laser intensity at the focus [30]. The profile of the polymerized structure is related to the square of laser intensity and the exposure time. With P2PP technique, microstructures that correspond to the positions where the intensity of diffracted beam is above the polymerization threshold are polymerized with one shot. This process can be seen as parallel polymerization with multilaser spots, where each laser spot corresponds to a white pixel of the designed pattern. The profile of the polymerized structure is a combined effect of ambient focal spots. The final radical density at the focal plane can be expressed as

$$\rho_{\text{facet}}(x,y,z) = \sum_{n=0}^{j}\sum_{m=0}^{k} \rho(x-n\Delta_x, y-m\Delta_y, z) \tag{3}$$

where $j$and k are the number of focal spots in the x and y direction, respectively; Δ_x and Δ_y are the intervals between laser spots in the x and y direction. The profile of polymerized structure can be achieved by solving

$$\rho_{\text{facet}}(x,y,z) > \rho_{\text{th}} \tag{4}$$

With longer exposure time and smaller interval, the area between focal spots will be fully polymerized. Thus, the profile of microstructures will be smoother.

In fact, the intensity distribution of laser pattern at the focal plane is not uniform. This is why the structures fabricated with curve patterns and plane patterns are not so uniform and deformed at the edge. The nonuniformity of the intensity distribution is caused by two factors. The first factor is the nonideality of the optical system. Quantized phase levels and finite resolution of SLM may cause phase distortion of laser beam. The high numerical aperture objective also produces aberration and leads to nonuniformity of intensity distribution. The second factor is the inaccuracy of the GS algorithm which is a numerical approximation algorithm. So, these may lead to the distortion of intensity distribution at the edge of laser pattern or in the whole laser pattern. Thus, the edge of microstructures will be rough or even deformed. Novel methods to improve the uniformity of intensity distribution should be further investigated.

4. Conclusion

In this paper, a P2PP fabrication system has been built and demonstrated by using SLM. Femtosecond laser beam has been modulated to curve patterns and plane patterns for efficient 2PP. With longer exposure time and smaller pixel distance, high surface smoothness of microstructure has been acquired. It was found that the distribution of laser intensity at the focal plane of objective has a significant effect on the profiles of microstructures. With P2PP fabrication technique, 2D or even 3D complex laser pattern can be fabricated with single exposure. The increased efficiency afforded by P2PP can make 2PP technique more viable for commercial use. Future work will concentrate on the promotion of uniformity of fabricated pattern and efficient fabrication of 3D structures with 2D and 3D laser patterns.

Acknowledgments

This work is supported by National Natural Science Foundation of China (Nos. 51275502 and 51205375), Anhui Provincial Natural Science Foundation (No.1408085ME104), National Basic Research Program of China (No. 2011CB302100), China Postdoctoral Science Foundation Funded Project (Nos. 2012M511416 and 2012M521245) and the Fundamental Research Funds for the Basic Researchniversities (KB2090090001). The authors would like to acknowledge the help of Parva Chhantyal from Laser Zentrum Hannover.

References

[1] Y.L. Zhang, Q.D. Chen, H. Xia, H.B. Sun, Nano Today 5 (2010) 435.
[2] V.FPlease provide page number for Ref.[2]. Paz, M. Emons, K. Obata, A. Ovsianikov, S. Peterhansel, K. Frenner, C. Reinhardt, B. Chichkov, U. Morgner, W. Osten, J. Laser Appl. 24 (2012).
[3] D.FPlease provide page number for Ref.[3]. Tan, Y. Li, F.J. Qi, H. Yang, Q.H. Gong, X.Z. Dong, X.M. Duan, Appl. Phys. Lett. 90 (2007).
[4] K. Takada, D. Wu, Q.D. Chen, S. Shoji, H. Xia, S. Kawata, H.B. Sun, Opt. Lett. 34 (2009) 566.
[5] A. Zukauskas, M. Malinauskas, C. Reinhardt, B.N. Chichkov, R. Gadonas, Appl. Opt. 51 (2012) 4995.
[6] VPlease provide page number for Ref.[6]. Melissinaki, A.A. Gill, I. Ortega, M. Vamvakaki, A. Ranella, J.W. Haycock, C. Fotakis, M. Farsari, F. Claeyssens, Biofabrication 3 (2011).
[7] D. Wu, Q.D. Chen, L.G. Niu, J.N. Wang, J. Wang, R. Wang, H. Xia, H.B. Sun, Lab Chip 9 (2009) 2391.
[8] W.S. Yan, M.M. Hossain, M. Gu, Opt. Lett. 38 (2013) 3177.
[9] L. Xiao-Feng, H. Guo-Qing, C. Qi-Dai, N. Li-Gang, L. Qi-Song, A. Ostendorf, S. Hong-Bo, Appl. Phys. Lett. 101 (2012) (113901)).
[10] T. Ergin, N. Stenger, P. Brenner, J.B. Pendry, M. Wegener, Science 328 (2010) 337.
[11] S.H. Park, D.Y. Yang, K.S. Lee, Laser Photon. Rev 3 (2009) 1.
[12] JPlease provide page number for Ref. [12]. Kato, N. Takeyasu, Y. Adachi, H.B. Sun, S. Kawata, Appl. Phys. Lett. 86 (2005).
[13] X.ZPlease provide page number for Ref.[13]. Dong, Z.S. Zhao, X.M. Duan, Appl. Phys. Lett. 91 (2007).
[14] Y. Yang, Q.Z. Li, G.P. Wang, Opt. Express 16 (2008) 11275.
[15] EPlease provide page number for Ref. [15]. Stankevicius, T. Gertus, M. Rutkauskas, M. Gedvilas, G. Raciukaitis, R. Gadonas, V. Smilgevicius, M. Malinauskas, J. Micromech. Microeng. 22 (2012).
[16] G. Bautista, M.J. Romero, G. Tapang, V.R. Daria, Opt. Commun. 282 (2009) 3746.
[17] C.F. Phelan, R.J. Winfield, D.P. O'Dwyer, Y.P. Rakovich, J.F. Donegan, J.G. Lunney, Opt. Commun. 284 (2011) 3571.
[18] S.D. Gittard, A. Nguyen, K. Obata, A. Koroleva, R.J. Narayan, B.N. Chichkov, Biomed. Opt. Express 2 (2011) 3167.
[19] Y.LPlease provide page number for the Ref.[19]. Hu, Y.H. Chen, J.Q. Ma, J.W. Li, W.H. Huang, J.R. Chu, Appl. Phys. Lett. 103 (2013).
[20] K. Obata, J. Koch, U. Hinze, B.N. Chichkov, Opt. Express 18 (2010) 17193.
[21] L. Kelemen, S. Valkai, P. Ormos, Opt. Express 15 (2007) 14488.
[22] H. Takahashi, S. Hasegawa, A. Takita, Y. Hayasaki, Opt. Express 16 (2008) 16592.
[23] Y.C. Li, L.C. Cheng, C.Y. Chang, C.H. Lien, P.J. Campagnola, S.J. Chen, Opt. Express 20 (2012) 19030.
[24] B. Mills, J.A. Grant-Jacob, M. Feinaeugle, R.W. Eason, Opt. Express 21 (2013) 14853.
[25] C.G. Xia, N.X. Fang, Biomed. Microdevices 11 (2009) 1309.
[26] C. Sun, N. Fang, D.M. Wu, X. Zhang, Sens. Actuator A—Phys. 121 (2005) 113.
[27] P.S. Salter, A. Jesacher, J.B. Spring, B.J. Metcalf, N. Thomas-Peter, R.D. Simmonds, N. K. Langford, I.A. Walmsley, M.J. Booth, Opt. Lett. 37 (2012) 470.
[28] J. Leach, K. Wulff, G. Sinclair, P. Jordan, J. Courtial, L. Thomson, G. Gibson, K. Karunwi, J. Cooper, Z.J. Laczik, M. Padgett, Appl. Opt. 45 (2006) 897.
[29] Z. Kuang, W. Perrie, D. Liu, P. Fitzsimons, S.P. Edwardson, E. Fearon, G. Dearden, K.G. Watkins, Appl. Surf. Sci. 258 (2012) 7601.
[30] J. Serbin, A. Egbert, A. Ostendorf, B.N. Chichkov, R. Houbertz, G. Domann, J. Schulz, C. Cronauer, L. Frohlich, M. Popall, Opt. Lett. 28 (2003) 301.